MOLECULAR IMAGING AND BIOLOGY

Mol Imaging Biol (2013) 15:649–654
DOI: 10.1007/s11307-013-0651-x

Published Online: 13 June 2013

World Molecular Imaging Society

BRIEF ARTICLE

Improved PET Imaging of Tumors in Mice Using a Novel ^{18}F-Folate Conjugate with an Albumin-Binding Entity

Cindy R. Fischer,[1] Viola Groehn,[2] Josefine Reber,[3] Roger Schibli,[1,3] Simon M. Ametamey,[1] Cristina Müller[3]

[1]*Center for Radiopharmaceutical Sciences of ETH, PSI and USZ, Institute of Pharmaceutical Sciences, ETH Zurich, 8093 Zurich, Switzerland*

[2]*Merck & Cie, 8200 Schaffhausen, Switzerland*

[3]*Center for Radiopharmaceutical Sciences of ETH, PSI and USZ, Paul Scherrer Institute, 5232 Villigen-PSI, Switzerland*

Abstract

Purpose: The folate receptor (FR) is a promising target for nuclear imaging due to its overexpression in many different cancer types. A drawback of using folate radioconjugates is the high accumulation of radioactivity in the kidneys. Therefore, the aim of this study was to develop a ^{18}F-labeled folate conjugate with an albumin-binding entity to enhance the blood circulation time and hence improve the tumor-to-kidney ratio.

Procedures: The novel ^{18}F-folate was prepared by conjugation of a ^{18}F-labeled glucose azide to an alkyne-functionalized folate precursor containing an albumin-binding entity via Cu(I)-catalyzed 1,3-dipolar cycloaddition. The radioconjugate was tested *in vitro* on FR-positive KB tumor cells and by biodistribution and positron emission tomography (PET) imaging studies using KB tumor-bearing mice.

Results: The radiosynthesis of the albumin-binding [^{18}F]fluorodeoxyglucose–folate ([^{18}F]3) resulted in a radiochemical yield of 1–2 % decay corrected (d.c.) and a radiochemical purity of ≥95 %. The specific activity of [^{18}F]3 ranged from 20 to 50 GBq/μmol. *In vitro* experiments revealed FR-specific binding of [^{18}F]3 to KB tumor cells. *In vivo* we found an increasing uptake of [^{18}F]3 into tumor xenografts over time reaching a value of ~15 % injected dose (ID)/g at 4 h post-injection (p.i.). Uptake in the kidneys (~13 % ID/g; 1 h p.i.) was approximately fourfold reduced compared to previously published ^{18}F-labeled folic acid derivatives. An excellent visualization of tumor xenografts with an unprecedentedly high tumor-to-kidney ratio (~1) was obtained by PET imaging.

Conclusions: [^{18}F]3 showed a favorable accumulation in tumor xenografts compared to the same folate conjugate without albumin-binding properties. Moreover, the increased tumor-to-kidney ratios improved the PET imaging quality significantly, in spite of a somewhat higher background radioactivity which was a consequence of the slower blood clearance of [^{18}F]3.

Key words: Folate receptor, Folic acid, Albumin-binding entity, PET, ^{18}F

Introduction

Overexpression of the folate receptor (FR) is found in many different cancer types as well as on the surface of activated macrophages, which are involved in inflammatory

Electronic supplementary material The online version of this article (doi:10.1007/s11307-013-0651-x) contains supplementary material, which is available to authorized users.

Correspondence to: Cristina Müller; *e-mail:* cristina.mueller@psi.ch

processes [1]. In healthy organs and tissues, the FR exists only at a few sites in polarized epithelia, for instance in the kidneys [2, 3]. In recent years, several folate-based radiotracers have been developed for nuclear imaging techniques such as positron emission tomography (PET) or single-photon emission computed tomography (SPECT) [4, 5]. However, a drawback of folate radioconjugates is a generally low tumor-to-kidney ratio as a result of significant accumulation of radioactivity in the kidneys. Therefore, several attempts were undertaken to reduce the kidneys uptake of folate radiopharmaceuticals [6–9]. Recently, it was shown that modification of antibody fragments with an albumin-binding entity resulted in increased tumor-to-kidney ratios as a consequence of their extended circulation time in the blood [10–12]. Encouraged by these excellent results, we wanted to apply this concept to our folate radioconjugates. Thus, a small molecular weight albumin-binding entity [13] was attached to a 1,4,7,10-tetraazacyclododecane-1,4,7,10-tetraacetic acid (DOTA) conjugate of folic acid with the aim to improve the tumor-to-kidney ratio as a consequence of an enhanced circulation time in the blood [14]. This novel DOTA–folate conjugate (cm09) was labeled with ^{177}Lu and tested in tumor-bearing mice. It showed an unprecedentedly high tumor uptake (18.1±1.80 % injected dose (ID)/g; 4 h post-injection (p.i.)) which was more than twice as high as for previously developed DOTA–folate conjugates without an albumin-binding entity [9, 15, 16]. Moreover, application of ^{177}Lu-cm09 resulted in a reduction of the renal uptake to 30 % of the value obtained with folate conjugates without an albumin-binding entity and led to a tumor-to-kidney ratio which was almost 1 [14].

In this study, we wanted to apply the strategy of increasing the circulation time of radiofolates to an ^{18}F-labeled folic acid conjugate for investigation of its *in vivo* characteristics in FR-positive KB tumor-bearing mice. For the design of such a novel folate radiotracer, one of our most successful ^{18}F-folate conjugates, [^{18}F]fluorodeoxyglucose (FDG)–folate [17], was selected as a basis for modification. An azide-derivatized ^{18}F-labeled glucose entity [18] was used as a prosthetic group. It was attached to a folate alkyne derivative with an albumin-binding entity as an additional functionality via Cu(I)-catalyzed 1,3-dipolar cycloaddition (Fig. 1). We hypothesized that this strategy would increase the tumor-to-kidney ratio and hence result in an improved tumor visualization using PET.

Material and Methods

Synthesis of Albumin-Binding [^{19}F]FDG-Folate (3)

The synthesis of 2-deoxy-2-fluoroglucopyranosyl azide (2) was performed according to the procedure described by Maschauer *et al.* [18]. Folate alkyne 1 was synthesized as described before [14]. To a solution of the folate alkyne (1, 20 mg, 21 µmol) in *t*-BuOH/H_2O (1:1, 1.2 ml), 2-deoxy-2-fluoroglucopyranosyl azide (2, 13.3 mg, 64 µmol), 0.1 M aqueous solution of $Cu(OAc)_2$ (0.1 Eq, 21 µl), and 0.1 M aqueous solution of sodium ascorbate (0.2 Eq, 43 µl) were added. The reaction mixture was stirred at room temperature for 1 h. The product was purified by semi-preparative HPLC (Supplementary Material). The desired fraction was collected and lyophilized to provide product 3 as a yellow powder (7.3 mg, 4.6 µmol, 21 %, purity according to HPLC of >92 %). HR-MS (ES^+) calculated for $C_{46}H_{56}FIN_{13}O_{13}$, 1,144.3144; found, 1,144.3139.

Radiosynthesis

The production of [^{18}F]fluoride is reported in the Supplementary Material. The synthesis of 2-deoxy-2-[^{18}F]fluoroglucopyranosyl azide ([^{18}F]2) was prepared according to a previously published procedure [17, 18]. An aqueous solution of 2-deoxy-2-[^{18}F]fluoroglucopyranosyl azide ([^{18}F]2) (0.5 ml) was added to the folate alkyne (1, 2 mg, 2.14 µmol) in DMF (0.4 ml) containing $Cu(OAc)_2$ (20 µl, 0.05 M) and sodium ascorbate (40 µl, 0.05 M). The reaction mixture was stirred at 50 °C for 15 min. Purification was achieved by semi-preparative radio-HPLC, followed by a reversed phase cartridge (Supplementary Material). The final product [^{18}F]3 was diluted with phosphate-buffered saline (PBS, pH 7.4, 0.5 ml) for *in vitro* and *in vivo* applications. Quality control was performed by analytical radio-HPLC (Supplementary Material, Fig. S1). The specific activity of [^{18}F]3 ranged from 20 to 50 GBq/µmol (Supplementary Material, Fig. S2).

Cell Culture and Cell Experiments

Culture of KB cells [19] (human cervical carcinoma cell line with a FR expression level; German Collection of Microorganisms and Cell Cultures, DSMZ, Braunschweig, Germany) and cell experiments are reported in the Supplementary Material.

Biodistribution Studies

All animal experiments were approved by the local veterinary department and complied with the Swiss and local laws on animal protection. Animals had free excess to food and water. Female CD-1 nude mice (Charles River, Germany) were fed with a folate-deficient rodent diet (Harlan Laboratories, USA). After an acclimatization period of 5–7 days, KB tumor cells (5×10^6 cells in 0.1 ml sterile PBS) were inoculated subcutaneously on both shoulders of each mouse. Twelve days later, the animals were intravenous (iv) injected with [^{18}F]3 (~3 MBq, 0.3 nmol, 100 µl). Blocking studies were performed with excess folic acid dissolved in PBS (100 µg in 100 µl) iv injected 5 min prior to [^{18}F]3. Animals were sacrificed at the indicated time points, and selected organs and tissues were collected, weighed, and measured in a γ-counter. The incorporated radioactivity was expressed as percentage injected dose [% ID] per gram of tissue. Statistical analyses were performed by using the unpaired two-tailed Student's *t* test (GraphPad Prism 6.0 Software). A P value of ≤0.05 was considered statistically significant.

PET/CT Imaging Studies

PET/CT experiments were performed with a dedicated small-animal PET/CT scanner (eXplore Vista PET/CT, GE). Animals

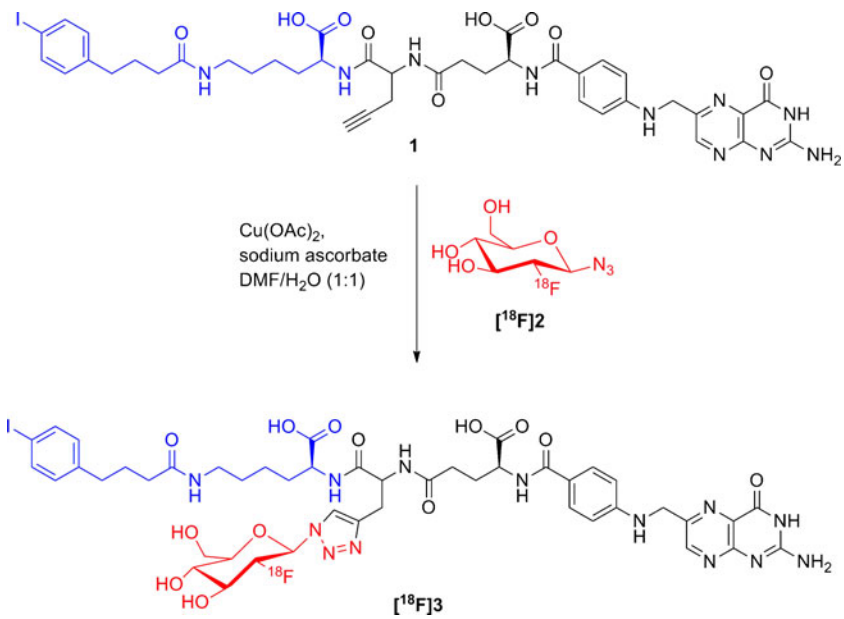

Fig. 1. Schematic radiosynthesis of the folate alkyne derivative 1 containing an albumin-binding entity (*blue*) with ^{18}F-labeled glucose azide (*red* ([^{18}F]2)) as a prosthetic group to obtain the albumin-binding [^{18}F]FDG-folate conjugate ([^{18}F]3).

were iv injected with [^{18}F]3 (~35 MBq, ~1.2 nmol, 100 µl). For scanning, mice were anesthetized with isoflurane in an air/oxygen mixture. The PET scans were acquired from 240 to 280 min p.i. followed by a CT. After acquisition, PET data were reconstructed in user-defined time frames, and the fused datasets of PET and CT were analyzed with the PMOD Software (version 3.4).

Results

Chemistry and Radiochemistry

The syntheses of the folate alkyne (1) and the 2-deoxy-2-fluoroglucopyranosyl azide (2) were previously reported in the literature [14, 18]. The Cu(I)-catalyzed cycloaddition of compounds 1 and 2 was performed in an aqueous solution. After semi-preparative HPLC purification, the nonradioactive reference compound 3 was obtained in a purity of >92 % and a yield of 21 %. The radiosynthesis of the albumin-binding [^{18}F]FDG-folate ([^{18}F]3) was performed in analogy to the previously published [^{18}F]fluorodeoxyglucose–folate [17]. [^{18}F]2 was obtained in 15–22 % radiochemical yield and was directly used for the "click reaction" with compound 1 to afford [^{18}F]3 in 15 % conversion. After HPLC purification and formulation for *in vivo* studies, [^{18}F]3 was obtained in an overall decay-corrected (d.c.) radiochemical yield of 1–2 % (n=7). The total synthesis time was 3 h, and [^{18}F]3 was obtained in a radiochemical purity of ≥95 %. Specific activity at the end of synthesis (EOS) ranged from 20 to 50 GBq/µmol. [^{18}F]3 was confirmed by co-injection of its nonradioactive reference compound 3 using analytical radio-HPLC. The log $D_{7.4}$ of [^{18}F]3 revealed a value of −3.2±0.4.

In Vitro Cell Experiments

The relative binding affinity of the nonradioactive reference compound 3 to FR-positive KB tumor cells revealed a value of 0.59±0.14 compared to folic acid which was set to 1. A value equal to that of folic acid indicates an equal affinity for the FR, a value lower than 1.0 reflects weaker affinity, and a value higher than 1.0 reflects stronger affinity [20, 21]. The folate derivative without albumin-binding entity, fluorodeoxyglucose–folate, showed a comparable value of 0.63±0.05 [17]. The displacement curve of one representative experiment for the albumin-binding compound 3 in comparison to the curve obtained for folic acid is shown in Fig. 2.

In addition, the cellular uptake of the radioactive folate conjugate [^{18}F]3 was investigated (Fig. 3). After incubation of [^{18}F]3 with KB tumor cells for 2 h at 37 °C, the uptake was about 65 % of the total added radioactivity, whereas the internalized fraction recorded for 29 % calculated per 0.3 mg protein. Co-incubation with excess folic acid resulted in a

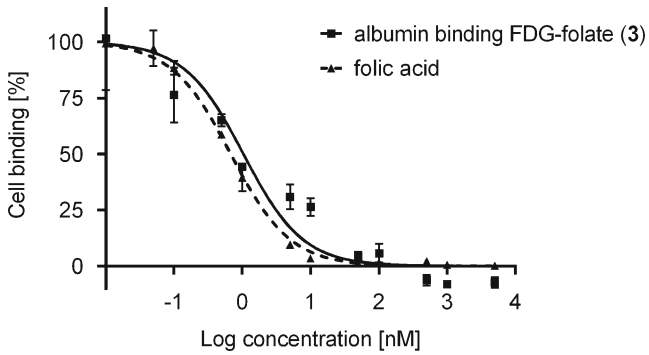

Fig. 2. Displacement curves of albumin-binding FDG-folate 3, fluorodeoxyglucose–folate, and folic acid using ^{3}H-folic acid and human FR-positive KB tumor cells.

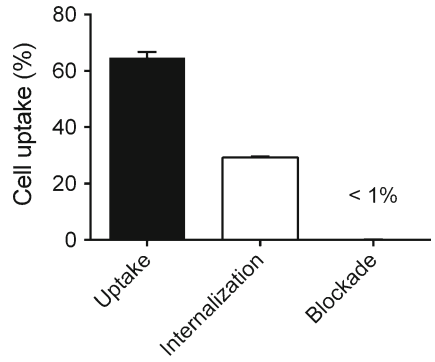

Fig. 3. *In vitro* study: uptake, internalization, and blockade of [^{18}F]3 in FR-positive KB cells, incubated at 37 °C for 2 h.

significant decline of radiotracer uptake to less than 1 % (Fig. 3).

Biodistribution Studies

The results of the biodistribution of [^{18}F]3 in KB tumor-bearing mice are shown in Table 1, including previously reported data of the radiotracer [^{18}F]fluorodeoxyglucose–folate that lacks the albumin-binding entity [17]. At 4 h p.i., the amount of radioactivity in the blood pool was still 2.21±0.15 % ID/g. Tumor uptake of [^{18}F]3 steadily increased over the measured time period (11.5±2.12 % ID/g, 1 h p.i.; 12.8±0.45 % ID/g, 2 h p.i.; 15.2±0.53 % ID/g, 4 h p.i.). After mice were co-injected with an excess folic acid, the uptake of [^{18}F]3 in FR-positive tumor xenografts was reduced by >75 % (4.16±0.43 % ID/g, 2 h p.i.). Specific uptake was also found in FR-positive tissues and organs such as the kidneys (17.4±1.14 % ID/g; 2 h p.i.) and salivary glands (7.76±1.26 % ID/g; 2 h p.i.) where the uptake was reduced by 83 % and 76 %, respectively, in mice which received excess folic acid. The tumor-to-kidney ratios were largely constant at a level of ~0.8 over the whole time of investigation. FR-unspecific accumulation of radioactivity was found in the liver (8.60±1.09 % ID/g; 2 h p.i.), gallbladder, and feces.

PET Imaging Studies

Figure 4 shows PET images as 3D projections of KB tumor-bearing mice injected with [^{18}F]3 (Fig. 4a) and the previously evaluated [^{18}F]fluorodeoxyglucose–folate (Fig. 4b). Both radiotracers were found to accumulate in FR-positive tumor xenografts, but the tumor uptake of [^{18}F]3 was increased, and the retention in the kidneys was clearly reduced compared to that of [^{18}F]fluorodeoxyglucose–folate. Hence, the tumor-to-kidney ratio of ~1 which was obtained with [^{18}F]3 was clearly higher than those for [^{18}F]fluorodeoxyglucose–folate. Excellent visualization of the tumor xenografts on both shoulders of the mouse injected with [^{18}F]3 was obtained in spite of the slower blood clearance of [^{18}F]3 compared to [^{18}F]fluorodeoxyglucose–folate. The uptake of [^{18}F]3 in nontargeted regions such as the intestinal tract and gallbladder was slightly more pronounced than in the case of [^{18}F]fluorodeoxyglucose–folate.

Discussion

Herein, we studied the implications of a chemical modification of a recently evaluated ^{18}F-based folate conjugate [17]

Table 1. Biodistribution data of albumin-binding [^{18}F]FDG-folate ([^{18}F]3) in nude mice bearing KB tumor xenografts in comparison to [^{18}F]fluorodeoxyglucose–folate [17]

	[^{18}F]FDG-folate ([^{18}F]3)[a]				[^{18}F]fluorodeoxyglucose–folate [17]	
	1 h p.i. (n=3)	2 h p.i. (n=3)	4 h p.i. (n=3)	2 h p.i. blockade[b] (n=3)	1 h p.i. (n=4)	1 h p.i. blockade[b] (n=3)
% ID/g						
Blood	8.20±1.73*	4.13±0.34	2.21±0.15	9.75±1.62	0.44±0.09*	1.37±1.80
Heart	4.60±1.02	3.37±0.10	2.54±0.19	3.46±0.38	1.15±0.13	1.66±2.05
Lungs	4.67±1.28	2.70±0.14	1.98±0.20	4.36±0.30	0.92±0.07	0.46±0.06
Spleen	1.48±0.21	1.10±0.12	0.75±0.06	1.32±0.20	0.73±0.21	0.23±0.05
Liver	9.34±0.61[n.s.]	8.60±1.09	5.64±0.62	2.33±0.44	9.49±1.13[n.s.]	10.0±3.53
Gallbladder	133.1±60.5	55.0±50.8	75.6±18.8	148.8±68.4	17.6±7.22	22.5±12.3
Kidneys	13.4±3.62*	17.4±1.14	18.1±0.41	3.02±0.16	42.9±2.04*	3.48±0.14
Stomach	2.26±0.41	1.72±0.12	1.48±0.03	1.20±0.15	1.42±0.53	0.33±0.08
Intestine	4.71±1.46	4.16±2.67	2.66±0.64	4.22±1.61	3.45±1.61	4.56±2.05
Feces	22.7±15.1	27.9±20.2	16.8±13.0	33.9±24.9	11.0±4.33	20.5±0.21
Salivary glands	6.72±0.96[n.s.]	7.76±1.26	6.37±0.33	1.89±0.41	5.93±0.77[n.s.]	0.30±0.01
Bone	1.62±0.14	1.42±0.23	1.13±0.05	1.15±0.23	0.87±0.05	0.29±0.01
Muscle	1.51±0.12	1.53±0.42	1.28±0.14	0.85±0.13	0.69±0.05	0.26±0.04
Tumor	11.5±2.12[n.s.]	12.8±0.45	15.2±0.53	4.16±0.43	10.0±1.12[n.s.]	1.19±1.04
Ratios						
Tumor/liver	1.25±0.30[n.s.]	1.50±0.15	2.70±0.21		1.06±0.02[n.s.]	
Tumor/kidneys	0.88±0.12*	0.73±0.03	0.84±0.04		0.23±0.04*	
Tumor/blood	1.42±0.18*	3.10±0.23	6.88±0.46		24.1±7.44*	

n.s. no statistical significance
*$P \leq 0.05$, statistically significant
[a]Approximately 3 MBq (0.3 nmol)
[b]Folic acid (100 μg) in PBS injected 5 min prior to [^{18}F]3

with the aim to improve the generally low tumor-to-kidney ratios of folate-based radiotracers. The radiosynthesis of a novel albumin-binding [^{18}F]FDG-folate [^{18}F]3 was performed in a similar manner to our previously published [^{18}F]fluorodeoxyglucose–folate [17]. The 1,3-dipolar cycloaddition to synthesize [^{18}F]3 was less efficient. Even after extension of the reaction time up to 30 min and increase of reaction temperature to 80 °C, the radiosynthesis of [^{18}F]3 proceeded in an overall radiochemical yield of 1–2 % (d.c.). Starting from 60 to 65 GBq of radioactivity, typical activities of 0.2–0.4 GBq of [^{18}F]3 were obtained. The lower yield obtained for [^{18}F]3 compared to [^{18}F]fluorodeoxyglucose–folate might be attributed to the steric hindrance by the albumin-binding entity of the folate alkyne derivative (1) with 2-deoxy-2-[^{18}F]fluoroglucopyranosyl azide ([^{18}F]2). Hence, the overall radiochemical yield could potentially be improved by introduction of a linker entity (*e.g.*, PEG spacer or short peptide chain) between the folate molecule and the albumin-binding entity. As expected, the introduction of the albumin-binding moiety resulted in a higher log $D_{7.4}$ value of −3.2±0.4 compared with [^{18}F]fluorodeoxyglucose–folate (log $D_{7.4}$, −4.2±0.1 [17]), indicating a slightly increased lipophilicity of [^{18}F]3 (Supplementary Material). *In vitro* cell experiments demonstrated FR-specific binding of [^{18}F]3 and retained high FR affinity of 3 comparable to that of native folic acid and fluorodeoxyglucose–folate. Biodistribution and PET imaging experiments performed with [^{18}F]3 confirmed the anticipated *in vivo* behavior of [^{18}F]3. Accumulation of [^{18}F]3 in the tumor tissue at 1 h p.i. did not significantly differ from the value found for the [^{18}F]fluorodeoxyglucose–folate without albumin-binding entity (Table 1 [17]). However, we found an increased tumor uptake of [^{18}F]3 at later time points after injection, reaching a high tumor accumulation of ~15 % ID/g at 4 h p.i. These findings were in contrast to the results obtained with fluorodeoxyglucose–folate which reached a maximum tumor uptake (~10 % ID/g) at 1 h after injection [17]. Moreover, retention of [^{18}F]3 in the kidneys was clearly reduced compared to the previously published [^{18}F]fluorodeoxyglucose–folate [17]. These circumstances resulted in tumor-to-kidney ratios which were unprecedentedly high for an ^{18}F-labeled folate conjugate. Due to the slow clearance of [^{18}F]3 from the blood, the retention of radioactivity was still about fourfold higher at 4 h p.i. (2.21±0.15 % ID/g) compared to the value found after injection of the ^{18}F-folate radiotracer without albumin-binding properties 1 h p.i. (0.44±0.09 % ID/g [17]). The relatively higher level of radioactivity in the blood due to the prolonged serum half-life of [^{18}F]3 resulted also in higher accumulation of radioactivity in nontargeted organs and tissues, such as the heart, lung, spleen, muscle, and gallbladder. Importantly, the FR-specific uptake in the kidneys (~13 % ID/g; 1 h p.i.; $P \leq 0.05$) was approximately fourfold reduced compared with previously published ^{18}F-labeled folic acid derivatives [17, 22, 23]. These findings are largely in agreement with the results found for ^{177}Lu-cm09 where the tissue distribution also showed a high uptake in the tumor and a reduced retention in the kidneys [14]. As expected, blocking experiments with an excess of folic acid resulted in a marked decrease of radioactivity accumulation in the tumors, kidneys, and salivary glands which proved the FR-specific uptake of [^{18}F]3 in these organs and tissues. The *ex vivo* biodistribution data obtained with [^{18}F]3 were confirmed by PET imaging studies whereby an increased target-to-nontarget contrast could be achieved compared to the previously reported [^{18}F]fluorodeoxyglucose–folate. A slightly more lipophilic character of [^{18}F]3 in comparison to [^{18}F]fluorodeoxyglucose–folate as a consequence of the albumin-binding entity favored hepatobiliary elimination, resulting in a higher accumulation of radioactivity in the gallbladder and abdominal region.

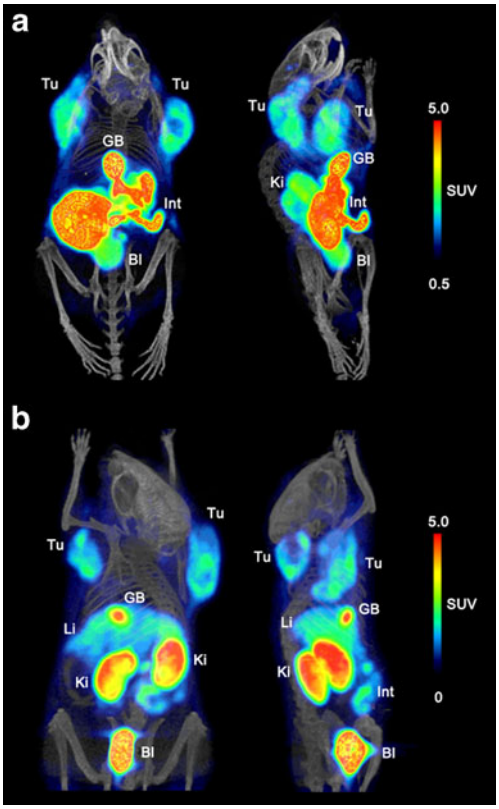

Fig. 4. Three-dimensional PET/CT images of KB tumor-bearing mice (*back and side views*): **a** mouse scanned 4 h after injection of [^{18}F]3 (~35 MBq, ~1.2 nmol); **b** mouse scanned 75 min after injection of [^{18}F]fluorodeoxyglucose–folate (~14 MBq, ~0.2 nmol). *Tu* tumor, *Ki* kidneys, *GB* gallbladder, *Bl* urinary bladder, *Int* intestines/feces, *Li* liver.

Conclusion

Our novel ^{18}F-labeled folic acid derivative [^{18}F]3 consists of a hydrophilic glucose entity as a radiolabeled prosthetic group and a small molecular weight albumin-binding entity. As a consequence of the albumin-binding properties, [^{18}F]3 showed an increased uptake in FR-positive tumors and an unprecedentedly high tumor-to-kidney ratio of almost 1. Enhancement of the blood circulation time is a valuable strategy not only for therapeutic application of folate

radiometal conjugates but also for diagnostic application using ^{18}F-based radiotracers.

Acknowledgments. We thank Dr. Thomas Betzel, Nadja Romano, and Martin Hungerbühler for their support and technical assistance. The project was financially supported by the Swiss National Science Foundation (Ambizione grants PZ00P3_121772 and PZ00P3_138834), COST-BM0607 (C08.0026), and the Swiss Cancer League (KLS-02762-02-2011).

Conflict of Interest. There are no conflicts of interest to declare.

References

1. Low PS, Henne WA, Doorneweerd DD (2008) Discovery and development of folic-acid-based receptor targeting for imaging and therapy of cancer and inflammatory diseases. Acc Chem Res 41:120–129
2. Parker N, Turk MJ, Westrick E et al (2005) Folate receptor expression in carcinomas and normal tissues determined by a quantitative radioligand binding assay. Anal Biochem 338:284–293
3. Birn H, Spiegelstein O, Christensen EI, Finnell RH (2005) Renal tubular reabsorption of folate mediated by folate binding protein 1. J Am Soc Nephrol 16:608–615
4. Ke CY, Mathias CJ, Green MA (2004) Folate-receptor-targeted radionuclide imaging agents. Adv Drug Deliv Rev 56:1143–1160
5. Müller C (2012) Folate based radiopharmaceuticals for imaging and therapy of cancer and inflammation. Curr Pharm Des 18:1058–1083
6. Müller C, Brühlmeier M, Schubiger AP, Schibli R (2006) Effects of antifolate drugs on the cellular uptake of radiofolates in vitro and in vivo. J Nucl Med 47:2057–2064
7. Müller C, Schibli R, Krenning EP, de Jong M (2008) Pemetrexed improves tumor selectivity of ^{111}In-DTPA-folate in mice with folate receptor-positive ovarian cancer. J Nucl Med 49:623–629
8. Reber J, Struthers H, Betzel T et al (2012) Radioiodinated folic acid conjugates: evaluation of a valuable concept to improve tumor-to-background contrast. Mol Pharm 9:1213–1221
9. Müller C, Vlahov IR, Santhapuram HK et al (2011) Tumor targeting using ^{67}Ga-DOTA-Bz-folate—investigations of methods to improve the tissue distribution of radiofolates. Nucl Med Biol 38:715–723
10. Dennis MS, Zhang M, Meng YG et al (2002) Albumin binding as a general strategy for improving the pharmacokinetics of proteins. J Biol Chem 277:35035–35043
11. Dennis MS, Jin H, Dugger D et al (2007) Imaging tumors with an albumin-binding Fab, a novel tumor-targeting agent. Cancer Res 67:254–261
12. Trüssel S, Dumelin C, Frey K et al (2009) New strategy for the extension of the serum half-life of antibody fragments. Bioconjug Chem 20:2286–2292
13. Dumelin CE, Trüssel S, Buller F et al (2008) A portable albumin binder from a DNA-encoded chemical library. Angew Chem Int Ed Engl 47:3196–3201
14. Müller C, Struthers H, Winiger C et al (2013) DOTA conjugate with an albumin-binding entity enables the first folic acid-targeted ^{177}Lu-radionuclide tumor therapy in mice. J Nucl Med 54:124–131
15. Müller C, Mindt TL, de Jong M, Schibli R (2009) Evaluation of a novel radiofolate in tumour-bearing mice: promising prospects for folate-based radionuclide therapy. Eur J Nucl Med Mol Imaging 36:938–946
16. Fani M, Wang X, Nicolas G et al (2011) Development of new folate-based PET radiotracers: preclinical evaluation of Ga-DOTA-folate conjugates. Eur J Nucl Med Mol Imaging 38:108–119
17. Fischer CR, Müller C, Reber J et al (2012) [^{18}F]Fluoro-deoxy-glucose folate: a novel PET radiotracer with improved in vivo properties for folate receptor targeting. Bioconjug Chem 23:805–813
18. Maschauer S, Prante O (2009) A series of 2-*O*-trifluoromethylsulfonyl-D-mannopyranosides as precursors for concomitant ^{18}F-labeling and glycosylation by click chemistry. Carbohydr Res 344:753–761
19. Jiang L, Zeng X, Wang Z, Chen Q (2009) Cell line cross-contamination: KB is not an oral squamous cell carcinoma cell line. Eur J Oral Sci 117:90–91
20. Leamon CP, Parker MA, Vlahov IR et al (2002) Synthesis and biological evaluation of EC20: a new folate- derived, ^{99m}Tc-based radiopharmaceutical. Bioconjug Chemistry 13:1200–1210
21. Reddy JA, Xu LC, Parker N, Vetzel M, Leamon CP (2004) Preclinical evaluation of ^{99m}Tc-EC20 for imaging folate receptor-positive tumors. J Nucl Med 45:857–866
22. Ross TL, Honer M, Müller C et al (2010) A new ^{18}F-labeled folic acid derivative with improved properties for the PET imaging of folate receptor-positive tumors. J Nucl Med 51:1756–1762
23. Betzel T, Müller C, Groehn V et al (2013) Radiosynthesis and preclinical evaluation of 3′-aza-2′-[^{18}F]fluorofolic acid: a novel PET radiotracer for folate receptor targeting. Bioconjug Chem 24:205–214